

## Nucleon strangeness and unitarity

M. J. Musolf

*Institute for Nuclear Theory, University of Washington, Seattle, Washington 98195*

H.-W. Hammer

*Institute for Nuclear Theory, University of Washington, Seattle, Washington 98195  
and Universität Mainz, Institut für Kernphysik, J.-J.-Becher Weg 45, D-55099 Mainz, Germany*

D. Drechsel

*Universität Mainz, Institut für Kernphysik, J.-J.-Becher Weg 45, D-55099 Mainz, Germany*

(Received 18 October 1996)

The strange-quark vector current form factors of the nucleon are analyzed within the framework of dispersion relations. Particular attention is paid to contributions made by  $K\bar{K}$  intermediate states to the form factor spectral functions. It is shown that, when the  $K\bar{K} \rightarrow N\bar{N}$  amplitude is evaluated in the Born approximation, the  $K\bar{K}$  contributions are identical to those arising from a one-loop calculation and entail a serious violation of unitarity. The mean square strangeness radius and magnetic moment are evaluated by imposing unitarity bounds on the kaon-nucleon partial wave amplitudes. The impact of including the kaon's strangeness vector current form factor in the dispersion integrals is also evaluated. [S0556-2821(97)05605-1]

PACS number(s): 14.20.Dh, 11.55.Fv, 12.38.Lg, 14.65.Bt

### I. INTRODUCTION

The low-energy structure of the nucleon's  $s\bar{s}$  sea has become a topic of serious study in the hadron structure community [1]. While deep inelastic scattering (DIS) has provided information about the light-cone momentum distribution of the strange sea [2], little is known about the corresponding spatial and spin distributions or about the role played by the sea in the nucleon's response to a low-energy probe. In an effort to study some of these low-energy characteristics of the sea, several semileptonic scattering experiments are underway and/or planned at MIT-Bates, TJNAF (formerly CEBAF), MAMI, and LANL. Parity-violating experiments using polarized electrons [3–8] are aimed primarily at probing nucleon matrix elements of the strange-quark vector current, which is parametrized by the strangeness electric and magnetic form factors  $G_E^{(s)}$  and  $G_M^{(s)}$ , respectively. Additionally, one expects the neutrino scattering data from LANL [9] to yield new limits on the strange-quark axial vector matrix element, characterized by the axial form factor  $G_A^{(s)}$ .

The corresponding problem for hadron structure theory is to compute these form factors and their leading moments, which depend crucially on nonperturbative aspects of QCD, in a credible manner. To this end, one may choose from a number of different strategies, each with its particular merits and limitations.

(a) Lattice QCD. To date, lattice calculations of the strangeness axial charge  $\Delta s = G_A^{(s)}(0)$  [10] and strangeness magnetic moment  $\mu^s = G_M^{(s)}(0)$  [11] have been carried out in the quenched approximation. The results for  $\Delta s$  are essentially consistent with the experimental value extracted from polarized DIS measurements [12]. The first lattice results for  $\mu^s$ , however, differ in sign from the preliminary experimental value obtained by the SAMPLE Collaboration [13]. With

the future development of more sophisticated lattice methods, one would anticipate better agreement between calculated and experimental values for these strangeness moments. The primary attraction of lattice calculations is that they provide the most direct, first principles, nonperturbative computations using QCD. By themselves, however, they may not provide as much insight as one would like into the mechanisms which govern the sign and scale of the strangeness form factors. Moreover, obtaining results for the non-leading  $Q^2$  dependence of the form factors may prove to be a formidable task.

(b) Effective theory. A complementary approach is to work with effective hadronic degrees of freedom rather than the quark and gluons of QCD, incorporating the underlying symmetries of the QCD Lagrangian into the effective hadronic Lagrangian. This approach, in the guise of chiral perturbation theory (CHPT), has seen considerable success in a variety of contexts [14]. A particular advantage of CHPT is its reliance on chiral symmetry and existing data, rather than on microscopic calculations, to determine quantities (chiral counterterms) whose values reflect the impact of short-distance hadronic interactions. Moreover, CHPT provides one with a useful language in which to describe the strong interaction dynamics responsible for the magnitude and sign of a particular quantity. In the case of the strangeness vector current form factors, however, CHPT cannot be used to make a model-independent prediction, as discussed in detail in Ref. [15].

(c) Hadronic models. A variety of model calculations for the strangeness form factors have been carried out [16–26], among which there appears little consensus as to the magnitude or sign of the different strangeness moments. Some models start from the effective theory framework and invoke additional model assumptions in order to arrive at predictions. Others, such as the cloudy bag model or nonrelativistic quark model, attempt to provide a more microscopic descrip-

tion of the form factors. The appeal of models is that they attempt to incorporate one's intuition about the physics which drives a particular aspect of hadron structure. Nevertheless, the correspondence between any model and the dynamics of QCD is open to debate. In the case of nucleon strangeness, this situation is reflected in the wide range of model predictions for strangeness form factors. If one wishes to understand the spin and spatial distribution of the  $s\bar{s}$  sea in terms of QCD, then models would appear to have a limited usefulness.

(d) Dispersion relations. In the present paper, we turn to this approach to try to derive insight into the strangeness form factors. The use of dispersion relations (DR's) has several merits, some of which are similar to those of effective theory. Like CHPT, DR's employ effective hadronic degrees of freedom rather than the quarks and gluons of QCD. Similarly, DR's offer a rigorous and, in principle, model-independent framework in which to understand the hadronic mechanisms which govern form factors. Both approaches attempt to relate experimental hadronic amplitudes to the form factors of interest, relying in the one case on chiral symmetry (CHPT) and in the other on analyticity and causality (DR's). Although DR's and CHPT are not QCD in a microscopic sense, they nevertheless embody QCD insofar as it is responsible for the experimental strong interaction observables used as input for a calculation.

For the present purposes, DR's offer additional advantages not afforded by CHPT. First, ultraviolet divergences can be eliminated using unitarity bounds rather than subtraction constants. In the case of the strangeness form factors, it is one's inability to determine the finite part of these counterterms which renders CHPT unproductive [15]. Second, DR's can be used to convert a given body of experimental data into predictions for the behavior of form factors over a range of momentum transfer. This situation contrasts with that of CHPT, which involves an expansion in powers of the external momentum and requires the determination of additional counterterms at each order in the expansion. The limitations of DR's, as an effective hadronic framework, are essentially set by the availability of sufficient data on strong and electroweak amplitudes. In the absence of such available data, one is forced, within this framework, to resort to ancillary approximations.

The application of DR's to the study of nucleon form factors is not new. Well before the discovery of QCD, DR's were used to analyze the nucleon electromagnetic (EM) form factors [27–29]. In addition to shedding light on the nucleon EM structure, dispersion relation analyses have allowed one to extract the couplings of various mesons to the nucleon [30,31]. More recently, DR's have been employed to make predictions for the nucleon's strange-quark vector current form factors [16,17,15]. These predictions have generally invoked the assumption of vector meson dominance, which, based on experience with the nucleon isovector EM form factor as well as on general grounds, is debatable. In principle, any nucleon form factor receives both resonant and nonresonant (continuum) contributions. In the case of the nucleon isovector EM charge radius, for example, the continuum contribution is non-negligible. While one can make a case for resonance dominance in the case of the nucleon mean square strangeness radius based on a model-dependent

extension of the effective theory approach [15], the logic rests on untested assumptions about the continuum contributions. Indeed, arriving at a rigorous, consistent, and model-independent analysis which incorporates both continuum and resonance contributions to the strangeness form factors remains an open problem for effective hadronic approaches.

With this problem in mind, we focus on the behavior of the multimeson continuum, emphasizing in particular the two-kaon contribution. The continuum contribution has been studied previously, with both CHPT and models, using one-loop kaon-strange baryon ( $B$ ) calculations [15,18–21,25]. In the  $t$  channel, such loops represent approximations to the  $K\bar{K}$  and  $B\bar{B}$  intermediate state contributions. Although the lightest intermediate state which can contribute to the form factors contains three pions, the  $KB$  loop calculations have been justified under the ansatz that hadronic states having valence  $s$  and  $\bar{s}$  quarks—the so-called “kaon cloud”—should give the dominant contribution. Using the  $K\bar{K}$  intermediate state as an illustrative example, we show how one-loop estimates of the continuum contribution can entail a serious violation of unitarity and evaluate the bounds on the continuum contribution which result from the imposition of unitarity. Our results indicate that effects which go beyond one-loop order—in effect, kaon rescattering corrections—cannot be neglected. We also analyze the impact on predictions for the nucleon strangeness form factors made by one's choice for the kaon strangeness form factor  $F_K^{(s)}$ . We find that this impact is nontrivial. Consequently, since  $F_K^{(s)}$  has not been measured, one's choice for its form necessarily introduces a certain degree of model dependence into the dispersion relation analysis. Finally, we note that the conclusions of the present study are provisional. We are unable to make any rigorous statements about contributions to the dispersion integrals in the kinematic regime where unitarity does not apply. In a subsequent paper we will report on our attempt to estimate these contributions by drawing upon existing kaon-nucleon scattering data. Similarly, we postpone to a future discussion any treatment of other multimeson continuum and baryon intermediate state contributions. In essence, our study follows the spirit of the analysis of Ref. [27]. In that work, the impact of unitarity constraints and inclusion of a pseudoscalar electromagnetic form factor were treated for the  $\pi\pi$  contribution to the nucleon isovector EM form factors.

Our discussion of these points is organized as follows. In Sec. II, we review the dispersion relation formalism as it applies to nucleon form factors. We also specify this formalism to the two-kaon continuum case, introducing our own version of the  $K\bar{K}$  partial waves to make unitarity constraints transparent. In Sec. III, we compare the two-kaon contribution in the Born approximation, which is equivalent to a one-loop calculation, with a calculation which incorporates the unitarity bounds and  $F_K^{(s)}$ . In Sec. IV we discuss our results for the mean-square strangeness radius and magnetic moment. Section V summarizes our conclusions and is followed by an appendix.

## II. FORMALISM

In writing down dispersion relations for the nucleon strangeness form factors, we find it useful to follow the treat-

ments of Drell and Zachariasen [32] and Federbush, Goldberger, and Treiman [27]. We also choose to work with the standard Dirac and Pauli form factors  $F_1^{(s)}$  and  $F_2^{(s)}$ , respectively, defined as

$$\langle N(p') | \bar{s} \gamma_\mu s | N(p) \rangle = \bar{U}(p') \left[ F_1^{(s)}(t) \gamma_\mu + \frac{i F_2^{(s)}(t)}{2m_N} \sigma_{\mu\nu} Q^\nu \right] U(p), \quad (1)$$

where  $U(p)$  is a spinor associated with the nucleon state  $|N(p)\rangle$ . Since the nucleon has no net strangeness, one has  $F_1^{(s)}(0) = 0$ . The form factors  $F_i^{(s)}$  ( $i=1,2$ ) are related to the Sachs electric and magnetic form factors [33] via

$$G_E^{(s)} = F_1^{(s)} - \tau F_2^{(s)}, \quad (2)$$

$$G_M^{(s)} = F_1^{(s)} + F_2^{(s)},$$

where  $t = Q^2 = (p' - p)^2$ ,  $\tau = -t/4m_N^2$  and  $p$  ( $p'$ ) is the initial (final) nucleon four-momentum. We are particularly interested in the leading moments associated with the  $F_i^{(s)}$ : the mean square strangeness radius and magnetic moment, defined as

$$\rho_D^s = \left. \frac{dF_1^{(s)}}{d\tau} \right|_{\tau=0}, \quad (3)$$

$$\mu^s = F_2^{(s)}(0). \quad (4)$$

We have chosen a dimensionless version of the mean-square radius, which is related to the corresponding dimensionful quantity as

$$\langle r_s^2 \rangle = 6 \left. \frac{dF_1^{(s)}}{dQ^2} \right|_{Q^2=0} = -\frac{3}{2} m_N^{-2} \rho_D^s. \quad (5)$$

In order to obtain a dispersion relation for one of the  $F_i^{(s)}(t)$  ( $i=1,2$ ), where  $t$  is real, one must assume that there exists an analytic continuation  $F_i^{(s)}(z)$  which approaches  $F_i^{(s)}(t)$  as  $z \rightarrow t + i\epsilon$ , which is analytic in the upper half plane and which has a branch cut on the real axis for  $t$  greater than some threshold  $t_0$ . In addition, one must assume that

$$\frac{F_i^{(s)}(z)}{z^n} \rightarrow 0, \quad (6)$$

as  $z \rightarrow \infty$ , anywhere in the upper half plane for some non-negative integer  $n$ . In this case, a straightforward application of Cauchy's theorem (using a circular contour excluding the branch cut) leads to the relations

$$F_i^{(s)}(t) = \frac{1}{\pi} \int_{t_0}^{\infty} \frac{\text{Im} F_i^{(s)}(t')}{t' - t - i\epsilon} dt' \quad (7)$$

in the case of  $n=0$ ,

$$F_i^{(s)}(t) - F_i^{(s)}(0) = \frac{t}{\pi} \int_{t_0}^{\infty} \frac{\text{Im} F_i^{(s)}(t')}{t'(t' - t - i\epsilon)} dt' \quad (8)$$

in the case of  $n=1$ , and so forth.

Employing as large a value of  $n$  as possible is desirable in order to improve the convergence of the function  $F_i^{(s)}(z)/z^n$  on the circular part of the contour at infinity. One has no way of knowing, *a priori*, which is the minimum value of  $n$  needed to guarantee that this contribution to the contour integral vanishes. The appropriate choice therefore remains one of the inherent uncertainties in the dispersion relation approach. It is conventional to use a subtracted dispersion relation [Eq. (8)] for the Dirac form factor ( $i=1$ ), since one knows on general grounds that the value of the form factor at  $t=0$  is just the charge associated with the corresponding current. In the case of  $\langle N(p') | \bar{s} \gamma_\mu s | N(p) \rangle$ , one has  $F_1^{(s)}(0) = 0$  since the nucleon carries no net strangeness. In the case of the magnetic form factor, one would like to predict its value at  $t=0$  rather than using it as a subtraction constant. Hence, we use the unsubtracted dispersion relation [Eq. (7)] for  $F_2^{(s)}(t)$ .

The essential physics content entering the DR's enters through the spectral functions  $\text{Im} F_i^{(s)}(t)$ . To analyze these spectral functions, we follow Refs. [27,32] and work in the  $N\bar{N}$  production channel, where the corresponding current matrix element is

$$\langle N(p); \bar{N}(\bar{p}) | \bar{s} \gamma_\mu s | 0 \rangle = \bar{U}(p) \left[ F_1^{(s)}(t) \gamma_\mu + \frac{i F_2^{(s)}(t)}{2m_N} \sigma_{\mu\nu} P^\nu \right] V(\bar{p}), \quad (9)$$

with  $P^\mu = (\bar{p} + p)^\mu$ ,  $t = P^2$ , and  $V(\bar{p})$  being an antinucleon spinor. In order to obtain the imaginary parts of the  $F_i^{(s)}$ , we reduce the antinucleon using the LSZ formalism and take the absorptive part. As in Refs. [27,32] the resulting contribution to the spectral functions arises from

$$\begin{aligned} & \text{Im} \langle N(p); \bar{N}(\bar{p}) | \bar{s} \gamma_\mu s | 0 \rangle \\ & \rightarrow \frac{\pi}{\sqrt{Z}} (2\pi)^{3/2} \mathcal{N} \sum_n \langle N(p) | \bar{J}_N(0) | n \rangle \\ & \quad \times \langle n | \bar{s} \gamma_\mu s | 0 \rangle V(\bar{p}) \delta^4(p + \bar{p} - p_n), \quad (10) \end{aligned}$$

where  $\mathcal{N}$  is a nucleon spinor normalization factor,  $Z$  is the nucleon's wave function renormalization constant, and  $\bar{J}_N(x) = J_N^\dagger(x) \gamma_0$  with  $J_N(x)$  being a nucleon source satisfying

$$(i\partial - m_N) \hat{\psi}_N(x) = J_N(x) \quad (11)$$

and with  $\hat{\psi}_N$  being the nucleon field. The content of the spectral function, as expressed in Eq. (10), has a useful diagrammatic representation as shown in Fig. 1.

The states  $|n\rangle$  of momentum  $p_n$  appearing in the sum are stable (with respect to the strong interaction). Consequently, no resonances appear in the sum, only asymptotic final states. In addition, the states  $|n\rangle$  must carry the same quantum numbers as the current  $\bar{s} \gamma_\mu s$ :  $I^G(J^{PC}) = 0^-(1^{--})$ . Moreover, owing to the presence of the source  $J_N(0)$ , they can have no net baryon number. In the purely mesonic sec-

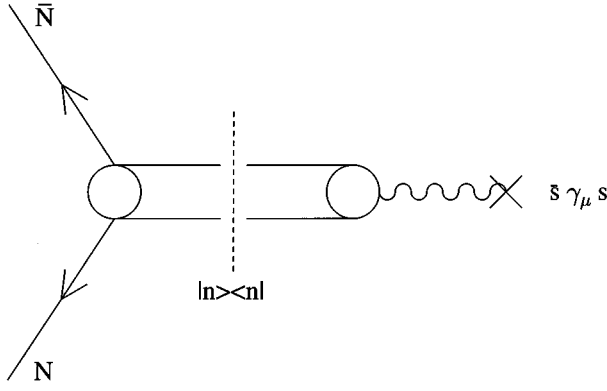


FIG. 1. Diagrammatic representation of the spectral decomposition for the nucleon strangeness vector current form factors given in Eq. (10). The right-hand part of the diagram denotes the matrix element to produce a  $I^G(J^{PC})=0^-(1^{--})$  state from the vacuum through the strangeness vector current. The left-hand side denotes the  $n \rightarrow N\bar{N}$  scattering amplitude.

tor, the lightest such states are  $3\pi$ ,  $5\pi$ ,  $7\pi$ ,  $2K$ ,  $9\pi$ ,  $KK\pi$ ,  $\dots$ . In the case of the baryons, one has  $N\bar{N}$ ,  $\Lambda\bar{\Lambda}$ ,  $\dots$ . One may also consider states containing both mesons and baryons, such as  $N\bar{N}\pi\pi$ . From this enumeration of states and the  $\delta$  function appearing in Eq. (10), one sees that the first cut in the dispersion integral appears at the  $3\pi$  production threshold  $t_0=9m_\pi^2$ . Higher-mass intermediate states generate additional cuts in the complex plane.

Many of the predictions for the  $F_i^{(s)}$  reported in the literature are based on approximations to the spectral functions appearing in Eqs. (7) and (8). In the work of Ref. [16], and updated in Ref. [17], a vector meson dominance approximation was employed, which amounts to assuming that one may write the spectral function as

$$\text{Im}F_i^{(s)}(t) = \pi \sum_j a_j \delta(t - m_j^2), \quad (12)$$

where  $j$  denotes a particular vector meson resonance (e.g.,  $\omega$ ,  $\phi$ ) and where the sum runs over a finite number of resonances. In terms of the formalism of Sec. II, this approximation omits any explicit mention of multimeson intermediate states  $|n\rangle$  and assumes that collectively the products  $\langle N(p)|\bar{J}_N(0)|n\rangle\langle n|\bar{s}\gamma_\mu s|0\rangle V(\bar{p})$  are strongly peaked in the regions near one or more vector meson masses.

In contrast, a variety of hadronic effective theory and model calculations have focused on contributions from the two-kaon intermediate state [15,18–21,25] even though it is not the lightest state appearing in the sum. The reason is based primarily on an intuition that kaons, which contain valence  $s$  or  $\bar{s}$  quarks, ought to give larger contributions to the matrix element  $\langle n|\bar{s}\gamma_\mu s|0\rangle$  than a purely pionic state in which there are no valence  $s$  or  $\bar{s}$  quarks. The validity of this ansatz is open to question for at least two reasons. First, the  $3\pi$  threshold is significantly below the  $K\bar{K}$  threshold. Consequently, the  $3\pi$  contribution will be weighted more strongly in the dispersion integral than the  $K\bar{K}$  contribution [owing to the denominators in Eqs. (7) and (8)]. Second, three pions can resonate into a state having the same quan-

tum numbers as the  $\phi$  (nearly pure  $s\bar{s}$ ) and, thereby, generate a nontrivial contribution to the current matrix element [34]. Indeed, the  $\phi$  has roughly a 15% branch to multipion final states (largely via a  $\rho\pi$  resonance). Although no resonances appear explicitly in the sum over states in Eq. (10), the impact of resonances nevertheless enters via the current matrix element  $\langle n|\bar{s}\gamma_\mu s|0\rangle$  and  $N\bar{N}$  production amplitude  $\langle N(p)|\bar{J}_N(0)|n\rangle V(\bar{p})$ . It is noteworthy that the kaon cloud predictions for  $\rho_D^s$  are typically smaller in magnitude than the vector meson dominance predictions and have the opposite sign.

We leave the relative size of the multipion and two-kaon contributions to a future study, and focus in the present paper on the two-kaon state. In doing so, our goal is to indicate how one-loop effective theory and model calculations which assume two-kaon dominance violate unitarity. In addition, we seek to illustrate the impacts on  $F_i^{(s)}$  predictions made by (a) the imposition of unitarity and (b) the inclusion of a form factor in the matrix element  $\langle n|\bar{s}\gamma_\mu s|0\rangle$ . To that end, we first decompose the  $K\bar{K} \rightarrow N\bar{N}$  amplitude into partial waves and relate them to the form factor spectral functions. We subsequently discuss possible parametrizations of the kaon strangeness form factor.

### A. Spectral functions, partial waves, and unitarity

By expanding the  $K\bar{K} \rightarrow N\bar{N}$  amplitude in partial waves, we are able to identify the pieces which contribute to the absorptive part of the nucleon current matrix element [Eq. (10)] and impose the constraints of unitarity in a straightforward manner. In doing so, it is convenient to follow the helicity amplitude formalism of Jacob and Wick [35]. We correspondingly assign the nucleon and antinucleon helicities  $\lambda_1$  and  $\lambda_2$ , respectively, and write the corresponding S-matrix element as

$$\begin{aligned} & \langle N(p, \lambda_1) \bar{N}(\bar{p}, \lambda_2) | \hat{S} | K(k_1) K(k_2) \rangle \\ &= (2\pi)^4 \delta^4(p + \bar{p} - k_1 - k_2) (2\pi)^2 \left[ \frac{64t}{t - 4m_K^2} \right]^{1/2} \\ & \times \langle \theta, \phi, \lambda_1, \lambda_2 | \hat{S}(P) | 00 \rangle, \end{aligned} \quad (13)$$

where  $P = p + \bar{p} = k_1 + k_2$ ,  $t = P^2$ , and  $m_K$  is the kaon mass. Defining

$$\begin{aligned} q_1^\mu &= \frac{1}{2}(k_1 - k_2)^\mu, \\ q_2^\mu &= \frac{1}{2}(\bar{p} - p)^\mu, \end{aligned} \quad (14)$$

we have  $(\theta, \phi)$  as the polar and azimuthal angles made by  $\vec{q}_2$  with respect to  $\vec{q}_1$  (the “|00>” indicates that the incoming mesons have no helicities and that we have chosen the  $z$  axis to be along  $\vec{q}_1$ ).

Following Ref. [35], we expand the matrix element  $\langle \theta, \phi, \lambda_1, \lambda_2 | \hat{S}(P) | 00 \rangle$  in partial waves as

$$\begin{aligned} S_{\lambda_1, \lambda_2} &\equiv \langle \theta, \phi, \lambda_1, \lambda_2 | \hat{S}(P) | 00 \rangle \\ &= \sum_J \left( \frac{2J+1}{4\pi} \right) b_J^{\lambda_1 \lambda_2} \mathcal{D}_{0\mu}^J(\phi, \theta, -\phi)^*, \end{aligned} \quad (15)$$

where  $\mathcal{D}_{\nu\nu'}^J(\alpha, \beta, \gamma)$  is the standard Wigner rotation matrix, where  $\mu = \lambda_1 - \lambda_2$  in Eq. (15) and where the  $b_J^{\lambda_1 \lambda_2}$  define the partial waves of angular momentum  $J$ .

Using the above definitions and imposing the requirement of unitarity on the  $S$  matrix,

$$S^\dagger S = 1, \quad (16)$$

one has that

$$|b_J^{\lambda_1, \lambda_2}| \leq 1 \quad (17)$$

for  $t \geq 4m_N^2$ .

In the expression for the spectral function appearing in Eq. (13), only the  $J=1$  partial waves appear since the states  $|n\rangle$  must carry the same quantum numbers as the current  $\bar{s}\gamma_\mu s$ . Moreover, it is well known that one has only two independent amplitudes for the scattering reaction  $KN \rightarrow KN$  and its crossed channel version  $K\bar{K} \rightarrow N\bar{N}$ . These amplitudes are commonly chosen to be the  $A$  and  $B$  amplitudes defined by the  $T$ -matrix element

$$\begin{aligned} T(-\bar{p}\lambda_1, k_1; p\lambda_2, -k_2) \\ = \bar{U}(p\lambda_2)[A + \frac{1}{2}B(k_1 - k_2)]V(\bar{p}\lambda_1), \end{aligned} \quad (18)$$

where we have employed crossing symmetry to obtain the  $t$ -channel version of the  $KN \rightarrow KN$  scattering amplitude. It is a straightforward exercise to relate the  $A$  and  $B$  amplitudes to the  $b_1^{\lambda_1 \lambda_2}$  [36]. We choose the two independent partial waves to correspond to  $(\lambda_1, \lambda_2) = (\frac{1}{2}, \frac{1}{2})$  and  $(\frac{1}{2}, -\frac{1}{2})$ . We obtain

$$\begin{aligned} b_1^{1/2, 1/2} = -\left(\frac{1}{2\pi}\right)\left(\frac{t-4m_K^2}{64t}\right)^{1/2} \left\{ \frac{p}{m_N} \int_{-1}^1 dx x A \right. \\ \left. - \frac{k}{2} \int_{-1}^1 dx (3x^2 - 1) B + \frac{k}{2} \int_{-1}^1 dx (x^2 - 1) B \right\}, \end{aligned} \quad (19)$$

$$b_1^{1/2, -1/2} = \left(\frac{1}{2\pi\sqrt{2}}\right)\left(\frac{t-4m_K^2}{64t}\right)^{1/2} \int_{-1}^1 dx \left(\frac{Ek}{m_N}\right) (1-x^2) B, \quad (20)$$

where  $x = \cos\theta$ ,  $k = |\vec{k}_1| = |\vec{k}_2|$ , and  $p = |\vec{p}| = |\vec{p}'|$  in the  $N\bar{N}$  c.m. frame, and  $E = \sqrt{p^2 + m_N^2}$ .

For future reference, we also note the following  $N\bar{N}$  production threshold relation between the partial waves:

$$b_1^{1/2, -1/2} = \sqrt{2} b_1^{1/2, 1/2}, \quad (21)$$

as  $t \rightarrow 4m_N^2$  (or  $P \rightarrow 0$ ). The origin of this relation is easy to understand. Since the  $N$  and  $\bar{N}$  have opposite intrinsic parities while the intrinsic parities of the  $K$  and  $\bar{K}$  are the same, the spin  $\times$  spatial part of the  $K\bar{K} \rightarrow N\bar{N}$  amplitude must transform as a pseudoscalar. In the  $K\bar{K}$  c.m. frame, one may therefore write the two independent amplitudes as

$$S_{\lambda_1, \lambda_2} = \chi_{\lambda_1}^\dagger [f_1 \vec{\sigma} \cdot \vec{k} + f_2 \vec{\sigma} \cdot \vec{p}] \chi_{\lambda_2}, \quad (22)$$

where  $\vec{k} \equiv \vec{k}_1$  and  $\vec{p} \equiv \vec{p}_1$  and where the functions  $f_i$  may depend on  $k^2$ ,  $\vec{k} \cdot \vec{p}$ , etc. At the threshold, one has  $\vec{p} = 0$ , so that only the amplitude proportional to  $f_1$  survives. From Eq. (22) we obtain

$$S_{1/2, 1/2} \rightarrow f_1 k_z = f_1 k \sqrt{\frac{4\pi}{3}} Y_{10}^*(\theta, \phi), \quad (23)$$

$$S_{1/2, -1/2} \rightarrow f_1 (k_x - ik_y) = -f_1 k \sqrt{\frac{8\pi}{3}} Y_{11}^*(\theta, \phi), \quad (24)$$

at the threshold ( $f_1$  may now only depend on  $k$ ). The partial waves are obtained by inverting Eq. (15), yielding

$$b_1^{1/2, 1/2} = 4\pi \sqrt{\frac{\pi}{3}} \int_{-1}^1 d\cos\theta Y_{10}(\theta, \phi) S_{1/2, 1/2}, \quad (25)$$

$$b_1^{1/2, -1/2} = -4\pi \sqrt{\frac{\pi}{3}} \int_{-1}^1 d\cos\theta Y_{11}(\theta, \phi) S_{1/2, -1/2}. \quad (26)$$

The foregoing expressions imply that the  $b_1^{\lambda_1, \lambda_2}$  are now independent of the angle  $\phi$ . Using the orthonormality of the spherical harmonics, one sees immediately from Eqs. (23)–(26) that the two partial waves are related at the threshold as indicated in Eq. (21).

We may now write the  $\text{Im}F_i^{(s)}(t)$  in terms of the two independent  $b_1^{\lambda_1, \lambda_2}$ . Starting from the general expression in Eq. (10), specifying the states  $|n\rangle$  to contain two kaons only, and replacing the sum  $\sum_n$  by appropriate integrals over two-kaon phase space, we obtain expressions for the spectral functions:

$$\begin{aligned} \text{Im}F_1^{(s)}(t) = \text{Re} \left\{ \left( \frac{m_N Q}{4P^2} \right) \left[ \frac{E}{\sqrt{2}m_N} b_1^{1/2, -1/2} - b_1^{1/2, 1/2} \right] \right. \\ \left. \times F_K^{(s)}(t)^* \right\} \end{aligned} \quad (27)$$

$$\text{Im}F_2^{(s)}(t) = \text{Re} \left\{ \left( \frac{m_N Q}{4P^2} \right) \left[ b_1^{1/2, 1/2} - \frac{m_N}{\sqrt{2}E} b_1^{1/2, -1/2} \right] F_K^{(s)}(t)^* \right\}, \quad (28)$$

where

$$P = \sqrt{t/4 - m_N^2}, \quad (29)$$

$$Q = \sqrt{t/4 - m_K^2}. \quad (30)$$

The kaon strangeness form factor  $F_K^{(s)}(t)$ , appearing in Eqs. (27) and (28), is defined through the matrix elements

$$\langle 0 | \bar{s}\gamma_\mu s | K^-(k_1) K^+(k_2) \rangle = (k_1 - k_2)_\mu F_K^{(s)}(t), \quad (31)$$

$$\langle 0 | \bar{s}\gamma_\mu s | \bar{K}^0(k_1) K^0(k_2) \rangle = (k_1 - k_2)_\mu F_K^{(s)}(t), \quad (32)$$

with  $F_K^{(s)}(0) = -1$ .

### B. Kaon strangeness form factor

The appearance of the kaon strangeness form factor  $F_K^{(s)}$  in expressions (27) and (28) necessarily implies the introduction of some model dependence into the dispersion relation analysis. The reason is that there exist no data on  $F_K^{(s)}(t)$ . Consequently, the best we can do is illustrate the impact of choosing a reasonable parametrization of this form factor. To this end, we first make a few general observations regarding  $F_K^{(s)}$  and its relationship to the  $K\bar{K}$  partial waves. In the product of  $F_K^{(s)}(t)^*$  and the partial waves  $b_1^{\lambda_1, \lambda_2}$  appearing in Eqs. (27) and (28), the real part will depend on both the magnitudes of these two factors as well as on their relative phase. Specifically, defining the phases as

$$b_1^{\lambda_1, \lambda_2} = |b_1^{\lambda_1, \lambda_2}| e^{i\delta_1}, \quad (33)$$

$$F_K^{(s)} = |F_K^{(s)}| e^{i\delta_K}, \quad (34)$$

one has

$$\begin{aligned} \text{Re}\{b_1^{\lambda_1, \lambda_2} F_K^{(s)}(t)^*\} &= |b_1^{\lambda_1, \lambda_2}| |F_K^{(s)}| \cos(\delta_1 - \delta_K) \\ &= |b_1^{\lambda_1, \lambda_2}| |F_K^{(s)}| (1 + \gamma_K), \end{aligned} \quad (35)$$

where we define a phase difference correction  $\gamma_K \equiv \cos(\delta_1 - \delta_K) - 1$ .

The lack of data on  $F_K^{(s)}$  is particularly problematic in seeking to determine  $\gamma_K$ . Here, the situation stands in contrast to the case of two-pion contributions to the nucleon's isovector EM form factors [30,31]. In the latter instance, the phase of the  $\pi\pi$  partial wave must be identical to that of the pion's isovector EM form factor for  $4m_\pi^2 \leq t \leq 16m_\pi^2$ . This feature follows from the fact that in this kinematic range, there is only one final state (involving two  $\pi$ 's) having the same quantum numbers as the isovector EM current. Unitarity then implies that the phase of the form factor and that of the scattering amplitude must be identical, that is, that the phase difference correction  $\gamma_\pi = 0$  [37]. In dispersion relation analyses of the isovector form factors one typically assumes that  $\gamma_\pi = 0$  everywhere below the  $N\bar{N}$  production threshold, since the phases associated with  $4\pi$ ,  $6\pi$ , etc., final states are small [38]. This latter practice falls under the rubric of "extended unitarity" [32,39,40]. In the case of  $K\bar{K}$  scattering, however, there exist several multipion final states which can be reached for  $t \geq 4m_K^2$ . Hence, there exists no regime in  $t$  for which  $\gamma_K = 0$ . At this time, we are unable to make any statements about  $\gamma_K$ , and we take its value to be one of the uncertainties in our analysis. We note, however, that  $|1 + \gamma_K| \leq 1$ . Thus, for purposes of setting an upper bound on the magnitude of the spectral function, we may set  $\gamma_K = 0$ .

In choosing our model parametrizations of  $F_K^{(s)}(t)$  we draw upon what is known about the lightest pseudoscalar meson form factors in the timelike region. First, it is well known that the pion EM form factor  $F_\pi(t)$  is dominated by the  $\rho$  resonance for  $4m_\pi^2 \leq t \leq (m_\pi + m_\omega)^2$  [41]. Moreover, more than 90% of the pion charge radius can be accounted for by the presence of a  $\rho$  pole [42]. The simplest parametrization which reproduces these gross features is that of the vector dominance model (VDM). The detailed structure of

$F_\pi(t)$ , including the shape of the  $\rho$  peak, requires more sophisticated parametrizations than that of  $\rho$  dominance [41]. Nevertheless, one is able to approximate the results of such analyses in the  $\rho$  region using a VDM parametrization with values for  $m_\rho$  and  $\Gamma_\rho$ , in good agreement with those obtained from other observables [41,43]. In the case of the kaon EM form factor  $F_K(t)$ , one has information in the timelike region from  $\sigma(e^+e^- \rightarrow K\bar{K})$  data [44]. As extracted from these data,  $F_K(t)$  displays a peak near the  $K\bar{K}$  threshold, which is also close to the value  $t = m_\phi^2$ . Conventional treatments of  $F_K(t)$  have correspondingly employed extended versions of the VDM, including poles associated with not only the  $\phi(1020)$ , but also the  $\rho$  and  $\omega$  [44]. For values of  $t \geq 2(\text{GeV}/c)^2$ , one begins to observe a bump-dip structure which cannot be reproduced using the three lightest vector mesons, and one is apparently forced to include poles associated with higher-mass vector mesons [44,45].

For our present purpose, it is sufficient to choose a parametrization for  $F_K^{(s)}(t)$  which produces behavior in the timelike region in reasonable accord with the gross structures of the pseudoscalar EM form factors. Indeed, we are not interested in obtaining airtight numerical predictions for the nucleon strangeness form factors, but rather in illustrating the impact which the use of a realistic  $F_K^{(s)}(t)$  has on these predictions. Hence, choosing a parametrization which produces the correct structure in detail is not necessary. Because the current  $\bar{s}\gamma_\mu s$  is purely isoscalar, we expect no significant contribution from  $1^+(1^{--})$  mesons<sup>1</sup> such as the  $\rho$ . The lightest  $0^-(1^{--})$  meson which might contribute is the  $\omega$ . However, we would expect the matrix element  $\langle \omega | \bar{s}\gamma_\mu s | 0 \rangle$  to be small since the  $\omega$  is nearly a pure  $(|u\bar{u}\rangle + |d\bar{d}\rangle)/\sqrt{2}$  state having a small admixture of  $|s\bar{s}\rangle$  at the level of  $\epsilon \approx 0.05$ . Consequently, we employ models which (a) are normalized to give the correct strangeness charge,  $F_K^{(s)}(0) = -1$ , and (b) contain a strong resonance enhancement in the vicinity of the  $\phi(1020)$ . The simplest such model is that of  $\phi$ -meson dominance, which yields

$$|F_K^{(s)}(t)_{\text{VDM}}| = \left\{ \frac{(\xi^2)^2 + m_\phi^2 \Gamma^2}{[(\xi^2 - t)^2 + m_\phi^2 \Gamma^2]} \right\}^{1/2}, \quad (36)$$

where  $\xi^2 \equiv m_\phi^2 - \Gamma^2/4$  and  $\Gamma$  is the width of the  $\phi(1020)$  resonance. An alternative is to adopt the Gounaris-Sakurai (GS) parametrization, which is reasonably successful in modeling  $F_\pi(t)$  in the  $\rho$ -peak region. When employing the GS form, we replace the  $\rho$  mass and width with those of the  $\phi$ . This parametrization can be found in Ref. [46] and we do not reproduce it here. It is interesting nevertheless to compare the VDM and GS forms near the  $\phi$  pole. Both can be shown to yield

<sup>1</sup>In short, we neglect isospin-breaking effects, such as  $\rho$ - $\omega$  mixing.

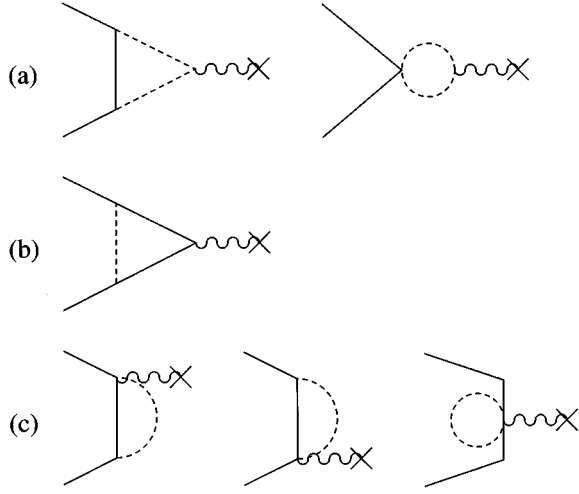


FIG. 2. One-loop diagrams for the strange vector form factors of the nucleon; the strange vector current  $\bar{s}\gamma_\mu s$  is denoted by the curly line, the dashed lines correspond to kaons, and the solid lines correspond to nucleons (external) or strange baryons (internal to loop).

$$|F_K^{(s)}(t=m_\phi^2)| = \frac{m_\phi}{\Gamma} + \delta, \quad (37)$$

where  $m_\phi/\Gamma \approx 255$ ,  $\delta_{\text{VDM}} \leq 0.01$ , and  $\delta_{\text{GS}} \approx -38$ . We also note that both models fall off to unity from their peak values at roughly the same place as  $F_K(t)$  [ $t \approx 2$  (GeV/c) $^2$ ]. In the following discussion, we compare predictions for the  $F_i^{(s)}(t)$  using the VDM and GS parametrizations with those obtained assuming pointlike behavior,  $F_K^{(s)}(t) \equiv -1$ .

### III. BORN APPROXIMATION AND BEYOND

Thus far, all calculations of the ‘‘kaon cloud’’ continuum contribution have been restricted to one-loop order. In the case of the nonlinear SU(3)  $\sigma$  model, for example, the relevant diagrams are shown in Fig. 2. Performing such a one-loop calculation is equivalent to (a) computing the amplitudes  $\langle N | \bar{J}_N | n \rangle V(\bar{p})$  and  $\langle n | \bar{s}\gamma_\mu s | 0 \rangle$  entering the expression in Eq. (10) under specific approximations and (b) using the resultant spectral functions in the appropriate dispersion integral of Eqs. (7) and (8). In particular, for loop contributions where the current is inserted on the kaon line [Fig. 2(a)], these approximations amount to computing the  $b_1^{\lambda_1, \lambda_2}$  in the Born approximation [see Fig. 3(a)] and taking the kaon strange form factor to be pointlike:  $F_K^{(s)} \equiv -1$  [see Fig. 4(a)]. For diagrams where the current is inserted on the strange baryon line [Fig. 2(b)], the corresponding approximations entail evaluating the  $B\bar{B} \rightarrow N\bar{N}$  amplitude in the one-meson exchange approximation [Fig. 3(b)] and taking the strange baryon strangeness form factor to be unity [Fig. 4(b)]. The remaining one-loop diagrams appearing in Fig. 2(c) are needed to guarantee that the one-loop amplitudes satisfy the Ward-Takahashi identity and have no analogue within the framework of DR’s. This equivalence between loops and DR’s has been discussed previously for the pion loop contribution to the nucleon isovector EM form factors in the context of the linear SU(2)  $\sigma$  model [27,28,32]. In what follows, we demonstrate the equivalence for the strangeness form fac-

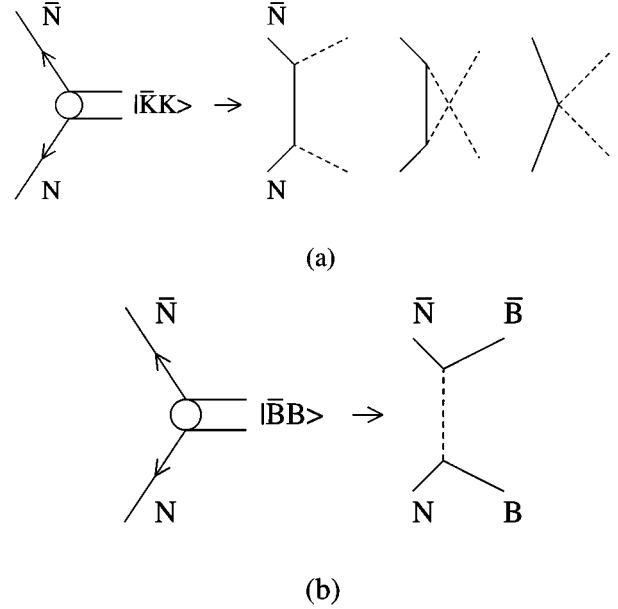


FIG. 3. Approximations for the  $n \rightarrow N\bar{N}$  scattering amplitude appearing in Fig. 1 and Eq. (10). Panel (a) gives the Born approximation for the  $K\bar{K} \rightarrow N\bar{N}$  amplitude, while (b) represents the  $B\bar{B} \rightarrow N\bar{N}$  amplitude in the one-meson exchange approximation ( $B$  is a baryon).

tors using the nonlinear SU(3)  $\sigma$  model [47,48]. We choose this model as it constitutes the standard paradigm of a chiral effective theory. We also show how, for the  $K\bar{K}$  contribution [Figs. 2(a) and 3(a)], the one-loop approximation is a rather drastic one.

In order to proceed, we first compute the  $b_1^{\lambda_1, \lambda_2}$  in the Born approximation (BA), using the amplitudes associated with the diagrams in Fig. 3(a). In the case of the baryon pole diagrams, we include only the  $\Lambda$  intermediate state since, in the limit of good SU(3) symmetry, the strong  $N\Sigma K$  coupling is highly suppressed with respect to the  $N\Lambda K$  coupling [49]. We obtain

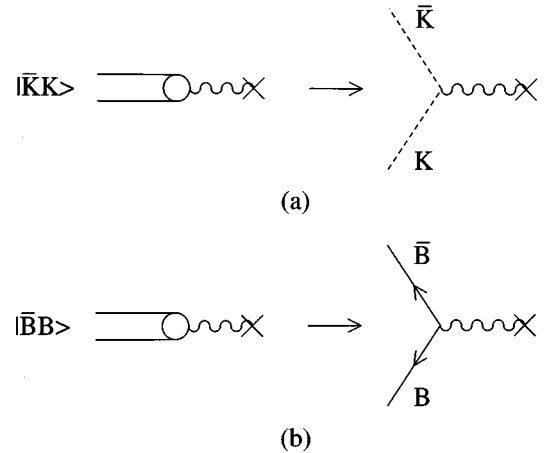


FIG. 4. Pointlike approximation for the matrix elements  $\langle n | \bar{s}\gamma_\mu s | 0 \rangle$  entering the spectral functions as in Eq. (10) and Fig. 1. Panel (a) corresponds to the pointlike kaon strangeness form factor, while (b) denotes the same for a baryon.

$$b_1^{1/2, 1/2} = \frac{1}{12\pi f^2} \left( \frac{2m_N Q^2}{\sqrt{t}} \right) \left\{ \frac{3}{2} - \frac{1}{6} (3F+D)^2 + \frac{1}{3} (3F+D)^2 \left( \frac{\bar{M}^2}{PQ} \right) [Q_0(x_B - i\epsilon) - Q_2(x_B - i\epsilon)] \right. \\ \left. + (3F+D)^2 \left( \frac{\bar{M}^2}{PQ} \right) Q_2(x_B - i\epsilon) + (3F+D)^2 \left( \frac{\bar{M}^2 \Delta \bar{M}}{Q^2} \right) Q_1(x_B - i\epsilon) \right\}, \quad (38)$$

$$b_1^{1/2, -1/2} = \frac{1}{12\pi f^2} \left( \frac{2\sqrt{2}EQ^2}{\sqrt{t}} \right) \left\{ \frac{3}{2} - \frac{1}{6} (3F+D)^2 + \frac{1}{3} (3F+D)^2 \left( \frac{\bar{M}^2}{PQ} \right) [Q_0(x_B - i\epsilon) - Q_2(x_B - i\epsilon)] \right\}, \quad (39)$$

where

$$x_B = \nu_p / \nu_0, \quad \nu_p = \nu_B + \bar{M} \Delta \bar{M}, \quad \nu_B = (t - 2m_K^2) / 4m_N \\ \nu_0 = PQ / m_N, \quad \bar{M} = (m_N + m_\Lambda) / 2, \quad \Delta \bar{M} = (m_\Lambda - m_N) / m_N, \quad (40)$$

where  $f \approx 93$  MeV is the pion decay constant, and where the  $Q_n(z)$  are Legendre functions of the second kind. The constants  $F$  and  $D$  are just the usual SU(3) reduced matrix elements, with  $D+F=1.26$  and  $F/D=0.64$ . Substituting these expressions into the formulas of Eqs. (27) and (28) yields

$$\text{Im}F_1^{(s)}(t) = \frac{1}{12\pi f^2} \left( \frac{Q^3}{2\sqrt{t}} \right) \text{Re}[F_K^{(s)}(t)] \left\{ \frac{3}{2} - \frac{1}{6} (3F+D)^2 + \frac{1}{3} (3F+D)^2 \left( \frac{\bar{M}^2}{PQ} \right) [Q_0(x_B) - Q_2(x_B)] \right. \\ \left. - (3F+D)^2 \frac{m_N^2}{P^2} \left[ \left( \frac{\bar{M}^2}{PQ} \right) Q_2(x_B) + \left( \frac{\bar{M}^2 \Delta \bar{M}}{Q^2} \right) Q_1(x_B) \right] \right\}, \quad (41)$$

$$\text{Im}F_2^{(s)}(t) = \frac{1}{12\pi f^2} \left( \frac{Q^3}{2\sqrt{t}} \right) \text{Re}[F_K^{(s)}(t)] (3F+D)^2 \frac{m_N^2}{P^2} \left[ \left( \frac{\bar{M}^2}{PQ} \right) Q_2(x_B) + \left( \frac{\bar{M}^2 \Delta \bar{M}}{Q^2} \right) Q_1(x_B) \right], \quad (42)$$

where we have made use of the fact that the  $b_1^{\lambda_1, \lambda_2}$  are real in the BA for  $t \geq 4m_K^2$ .

After setting  $F_K^{(s)}(t) \equiv -1$  in Eqs. (41) and (42), one obtains expressions for the spectral functions which are identical to those obtained from the Feynman amplitudes associated with the diagrams in Fig. 2(a). To see how this equivalence comes about, we refer to the analytic structure of the matrix element  $\langle N(p); N(\bar{p}) | \bar{s} \gamma_\mu s | 0 \rangle$ . Any discontinuities across the real  $t$  axis must arise from integration over poles associated with the presence of one of the physical states  $|n\rangle$  appearing in Eq. (10). The Cutkosky rules [50,51] give a procedure for extracting these discontinuities from Feynman amplitudes. In particular, we may obtain the corresponding discontinuity from the Feynman amplitudes by making the following replacement for each propagator associated with one of the particles appearing in the given state  $|n\rangle$ :

$$\frac{1}{p^2 - m^2 + i\epsilon} \rightarrow -2\pi i \theta(p_0) \delta(p^2 - m^2). \quad (43)$$

Since the only state  $|n\rangle$  contained in the loops of Fig. 2(a) is  $|K\bar{K}\rangle$ , we make the replacement of Eq. (43) for the two-kaon propagators in the loop integrals. Doing so, and carrying out the loop integration, yields the formulas in Eqs. (41) and (42). The details of this procedure are shown in the Appendix. Thus, insofar as the DR's of Eqs. (7) and (8) are valid,

the use of one-loop amplitudes and the use of Eq. (10) with the BA for the  $K\bar{K} \rightarrow N\bar{N}$  amplitudes are equivalent.

With explicit formulas for the spectral functions in hand, it is now straightforward to carry out the dispersion integrals. When the nonlinear SU(3)  $\sigma$  model is used to perform one-loop calculations for these leading moments, one finds that  $\rho_D^s$  contains a UV divergence. Using the dispersion relation framework, we correspondingly find that the  $K\bar{K}$  contribution to  $\rho_D^s$  is divergent in the dispersive variable  $t$  when the BA is used to compute the  $b_1^{\lambda_1, \lambda_2}$  and a pointlike kaon strangeness form factor is employed. In the case of loops, this UV divergence can be handled in a variety of ways. When one attempts an analysis using CHPT, the divergence is removed by the corresponding counterterm. This counterterm, however, contains a finite remainder which cannot be determined in any model-independent way from existing measurements [15]. Consequently, one must invoke additional model-dependent assumptions in order to make predictions using loops. A variety of such scenarios are discussed and evaluated in Ref. [15]. These alternatives include assuming that the finite low-energy constants in CHPT are saturated by vector meson resonances or assuming that the loop integrals are cut off by form factors and the meson-baryon vertices. Each involves a departure from QCD (at the level of hadronic effective theory) to a greater or lesser extent and entails a certain amount of ambiguity. Ideally, one would like to find a less model-dependent way of regulating the UV behavior of the integrals and obtaining a finite prediction.



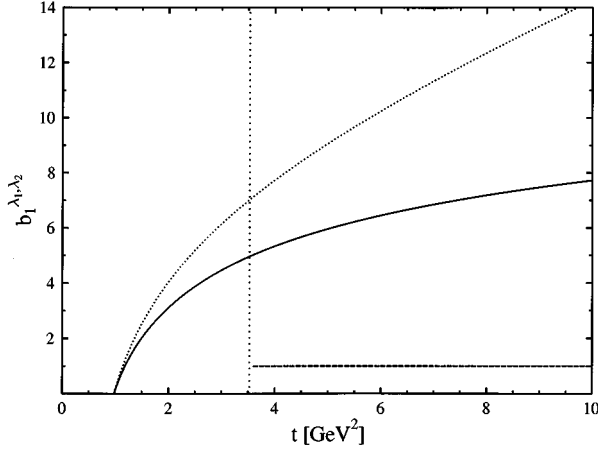


FIG. 5. Partial waves  $b_1^{\lambda_1, \lambda_2}$  for  $KN$  scattering in the nonlinear  $SU(3)$   $\sigma$  model. The solid and dotted lines correspond to  $b_1^{1/2, 1/2}$  and  $b_1^{1/2, -1/2}$ , respectively. The dashed line shows the unitarity bound on  $b_1^{1/2, -1/2}$ ; the bound on  $b_1^{1/2, 1/2}$ , which is not shown, is a factor of  $1/\sqrt{2}$  smaller at the  $NN$  threshold, indicated by the vertical dotted line.

In the present context, the unitarity bound on the partial waves [Eqs. (19) and (20)] provides such a model-independent regulator. The physical amplitudes  $b_1^{\lambda_1, \lambda_2}$  must satisfy the bound [Eq. (17)], regardless of one's model for  $KN$  scattering. To illustrate the impact of the unitarity bound, we plot in Fig. 5 the partial waves computed in the BA as a function of  $t$  and the corresponding unitarity bound above the two-nucleon threshold. One sees that the  $b_1^{\lambda_1, \lambda_2}$  in the BA violate the unitarity bound by a factor of 4 or more at the threshold and that this violation grows with  $t$ .

When translating the unitarity bound into a bound on the spectral functions, some care is required. The most naive approach is to begin with Eqs. (27) and (28), apply the triangle inequality, and take  $|b_1^{\lambda_1, \lambda_2}| = 1$ , viz.,

$$\begin{aligned} |\text{Im}F_1^{(s)}(t)| &\leq \left( \frac{m_N Q}{4P^2} \right) \left| \frac{E}{\sqrt{2}m_N} b_1^{1/2, -1/2} - b_1^{1/2, 1/2} \right| |F_K^{(s)}(t)|^* \\ &\leq \left( \frac{m_N Q}{4P^2} \right) \left\{ \frac{E}{\sqrt{2}m_N} |b_1^{1/2, -1/2}| + |b_1^{1/2, 1/2}| \right\} \\ &\quad \times |F_K^{(s)}(t)|, \end{aligned} \quad (44)$$

and similarly for  $|\text{Im}F_2^{(s)}(t)|$ . In arriving at the first line of Eq. (44) we have set the phase difference correction  $\gamma_K = 0$  as discussed previously. Setting  $|b_1^{\lambda_1, \lambda_2}| = 1$  and using  $t = \sqrt{2}E$  in the  $NN$  c.m. frame, we obtain the naive unitarity bounds

$$|\text{Im}F_1^{(s)}(t)| \leq \frac{Q}{8\sqrt{2}P^2} (2\sqrt{2}m_N + \sqrt{t}) |F_K^{(s)}(t)|, \quad (45)$$

$$|\text{Im}F_2^{(s)}(t)| \leq \frac{m_N Q}{4\sqrt{2}tP^2} (\sqrt{2t} + 2m_N) |F_K^{(s)}(t)|. \quad (46)$$

These naive bounds [Eqs. (45) and (46)] are shown in Fig. 6

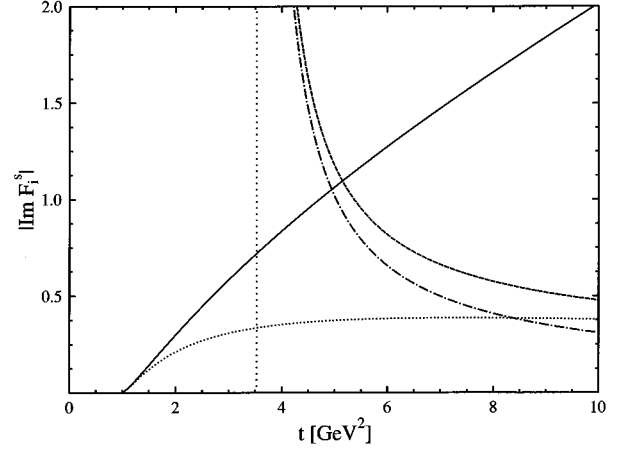


FIG. 6. Spectral functions in the nonlinear  $\sigma$  model and naive unitarity bounds. A pointlike strangeness form factor for the kaon has been used. The solid and dotted lines show the results for  $\text{Im}F_1^{(s)}(t)$  and  $\text{Im}F_2^{(s)}(t)$ , respectively. The corresponding naive unitarity bounds are indicated by the dashed and dash-dotted lines, respectively. The vertical dotted line indicates the two-nucleon threshold.

together with the BA where a pointlike strangeness form factor for the kaon has been applied. The divergence in these bounds appearing at the  $NN$  threshold arises from the  $1/P^2$  factor appearing in Eqs. (45) and (46). The presence of this singularity renders the functions appearing in the right-hand side (RHS) of Eqs. (45) and (46) nonintegrable over the range  $4m_N^2 \leq t \leq \infty$ . Thus, the naive bounds are not meaningful.

A more careful application of unitarity requires that one also take into account the threshold relation on the  $b_1^{\lambda_1, \lambda_2}$  appearing in Eq. (21). This relation forces the linear combinations of  $b_1^{\lambda_1, \lambda_2}$  appearing in Eqs. (27) and (28) to go as  $P^2$  near the threshold, thereby ensuring that the spectral functions are finite as  $P \rightarrow 0$ . Hence, when imposing unitarity, one must enforce the threshold relation. For simplicity, we choose to take  $b_1^{1/2, 1/2} = b_1^{1/2, -1/2}/\sqrt{2}$  everywhere above  $4m_N^2$ , even though this relation rigorously applies only at  $t = 4m_N^2$ , and take  $|b_1^{1/2, -1/2}| \leq 1$ . This leads to the bounds

$$|\text{Im}F_1^{(s)}(t)| \leq \frac{Q}{2\sqrt{2}(\sqrt{t} + 2m_N)} |F_K^{(s)}(t)|, \quad (47)$$

$$|\text{Im}F_2^{(s)}(t)| \leq \frac{m_N Q}{\sqrt{2}t(\sqrt{t} + 2m_N)} |F_K^{(s)}(t)|, \quad (48)$$

which now can be used in the dispersion relations (7) and (8) without ambiguity. Furthermore, the bounds with the correct threshold behavior built in are always more stringent than the naive ones for all  $t \geq 0$ . Figure 7 shows these bounds [Eqs. (47) and (48)] together with the BA and a pointlike kaon strangeness form factor in both cases. We show only the bound on  $|\text{Im}F_1^{(s)}(t)|$ , since  $|\text{Im}F_2^{(s)}(t)| \leq |\text{Im}F_1^{(s)}(t)|m/E$ . It is clear from the curves in Fig. 7 that unitarity has a significant impact on the spectral functions above the  $NN$  threshold.

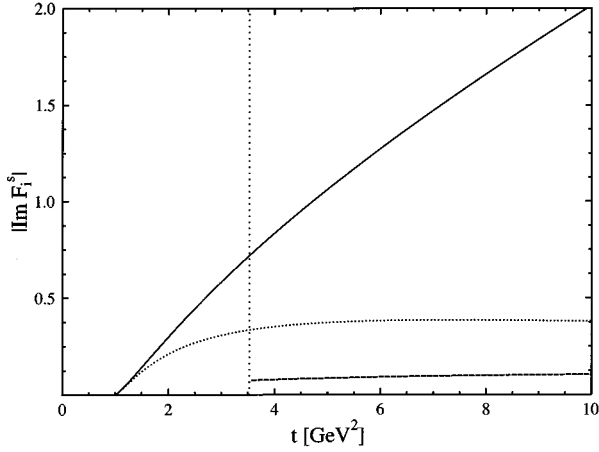


FIG. 7. Same as Fig. 6 but with the *correct* unitarity bounds of Eqs. (47) and (48). The bound on  $\text{Im}F_2^{(s)}(t)$  is not displayed because it is even more stringent than the bound on  $\text{Im}F_1^{(s)}(t)$ .

In addition to correcting the  $K\bar{K} \rightarrow N\bar{N}$  in the BA for unitarity, we also attempt a more realistic treatment of the kaon strangeness form factor appearing in Eqs. (27) and (28). As discussed above, we do so by choosing two parametrizations strongly peaked in the vicinity of the  $\phi(1020)$  resonance. In Fig. 8 we plot the same quantities as in Fig. 7 but using the GS form factor. For  $4m_K^2 \leq t \leq 4m_N^2$ , the  $\phi$  peak in the GS parametrization leads to a strong enhancement of the spectral functions as compared with the use of a pointlike form factor. As  $t$  increases beyond the  $N\bar{N}$  threshold, the GS form factor eventually suppresses the spectral functions when either the BA or unitarity bounds are used. The impact of using the simpler VDM parametrization is similar to that of the GS form factor. Although we could have attempted to carry out a more detailed analysis of  $F_K^{(s)}(t)$ , the plot in Fig. 8 makes the essential point clear: The impact of choosing a reasonable nonpointlike form for  $F_K^{(s)}(t)$  can be nontrivial.

#### IV. STRANGENESS MOMENTS

In this section, we explore the numerical consequences of unitarity and  $F_K^{(s)}(t)$  parametrization for the leading strange-

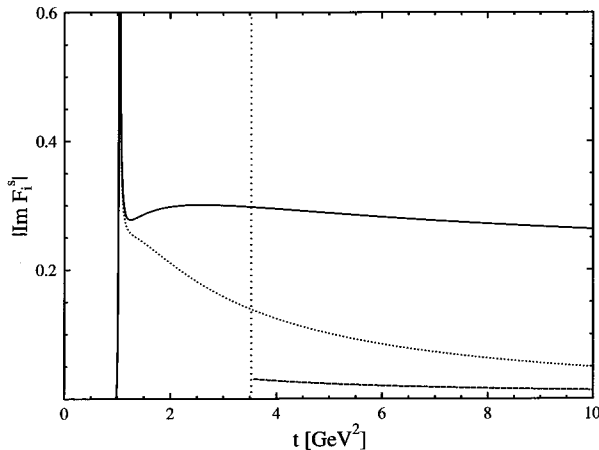


FIG. 8. Same as Fig. 7 but using the GS parametrization for the kaon strangeness form factor, peaked for  $\sqrt{t} \approx m_\phi$ . Note the difference in vertical scale as compared to Figs. 6 and 7.

TABLE I. Contributions from kaon intermediate state to the nucleon strangeness radius and magnetic moment, computed using dispersion relations. Results are given using three different scenarios as discussed in the text: (a) BA/PFF, partial waves  $b_1^{\lambda_1, \lambda_2}$  computed in BA and kaon strangeness form factor  $F_K^{(s)}(t) \equiv -1$ ; (b) BA/U/PFF, same as (a) but with unitarity limit from Eqs. (47) and (48) applied for  $t \geq 4m_N^2$ ; (c) BA/U/GS, same as (b) but with Gounaris-Sakurai parametrization for  $F_K^{(s)}(t)$ . To convert  $\rho_D^s$  to  $\langle r_s^2 \rangle$ , multiply  $\rho_D^s$  by  $-0.066 \text{ fm}^2$ .

Moment	Scenario	$4m_K^2 \leq t \leq 4m_N^2$	$4m_N^2 \leq t$	Total
$\rho_D^s$	BA/PFF	0.18	div	div
	BA/U/PFF	0.18	0.03	0.21
	BA/U/GS	0.26	0.01	0.27
$\mu^s$	BA/PFF	-0.07	-0.40	-0.47
	BA/U/PFF	-0.07	-0.07	-0.14
	BA/U/GS	-0.09	-0.01	-0.10

ness moments  $\rho_D^s$  and  $\mu^s$ . For purposes of later discussion, it is useful to write down the DR's for these two quantities:

$$\rho_D^s = -\frac{4m_N^2}{\pi} \int_{4m_K^2}^{\infty} dt \frac{\text{Im}F_1^{(s)}(t)}{t^2}, \quad (49)$$

$$\mu^s = \frac{1}{\pi} \int_{4m_K^2}^{\infty} dt \frac{\text{Im}F_2^{(s)}(t)}{t}. \quad (50)$$

Using these expressions, we compare three scenarios for computing the  $K\bar{K}$  contribution to the moments: (a) a calculation using the BA for the  $b_1^{\lambda_1, \lambda_2}$  and pointlike kaon strangeness form factor (BA/PFF), (b) the same as (a) but imposing the unitarity bounds of Eqs. (47) and (48) for  $t \geq 4m_N^2$  (BA/U/PFF), and (c) the same as (b) but using the GS parametrization for  $F_K^{(s)}(t)$  (BA/U/GS). Of these scenarios, we recall that (a) is equivalent to computing the one-loop amplitudes of Fig. 2(a). We further delineate between the contributions to the dispersion integrals in Eqs. (8) and (7) arising from the integration regions  $4m_K^2 \leq t \leq 4m_N^2$  and  $4m_N^2 \leq t$ . In applying the unitarity bound [scenarios (b) and (c)], we assume for simplicity that the spectral functions do not change sign across the two-nucleon threshold and that this sign is given by the phase of the spectral function for  $t \leq 4m_N^2$ . The results are given in Table I. From the entries in the table, the numerical impact of imposing unitarity and choosing a nonpointlike form factor is evident. In the case of  $\rho_D^s$ , unitarity eliminates the UV divergence and sets a bound on the contribution from the region above the  $N\bar{N}$  threshold which is small. In terms of the dimensionful Dirac radius, this contribution is about  $-0.002 \text{ fm}^2$ . The use of the GS parametrization for  $F_K^{(s)}(t)$ , on the other hand, increases the contribution from the region  $4m_K^2 \leq t \leq 4m_N^2$  by about 50%, owing largely to the  $\phi$  peak near the two-kaon threshold. Even though the  $F_1$  spectral function with the GS form factor falls below the corresponding spectral function with a pointlike form factor for  $t > 2 \text{ (GeV}/c)^2$ , the  $1/t^2$  appearing in the integrand of Eq. (49) favors the contribution from the

region containing the  $\phi$ -resonance enhancement. Consequently, the reduction for  $2(\text{GeV}/c)^2 \leq t \leq 4m_N^2$  is not significant.

For the strange magnetic moment, the BA contribution with a pointlike  $F_K^{(s)}(t)$  yields a finite result, in contrast to the situation with  $\rho_D^s$ . Nevertheless, the imposition of unitarity reduces the  $t \geq 4m_N^2$  contribution to one-sixth of its BA value. Insofar as the contribution from this region was the dominant one in the BA, this unitarity reduction is quite significant. The use of the GS form factor reduces this contribution even further, whereas its impact in the region  $4m_K^2 \leq t \leq 4m_N^2$  is small. In the latter instance, the enhancement from the  $\phi$  peak is not as important as in the case of  $\rho_D^s$ , since the integrand in Eq. (50) only weights the low- $t$  behavior as  $1/t$ .

We emphasize that, although the results listed in the last column of Table I may be instructive, one should not take the precise numerical values too seriously. It is clear from the results in the fourth column, as well as from the curves in Figs. 5, 7, and 8, that the consequences of the unitarity constraints are significant. The physical mechanisms responsible for the reduction of the  $b_1^{\lambda_1, \lambda_2}$  and  $\text{Im}F_i^s$  from their BA values to the unitarity limits—primarily nonresonant and resonant kaon rescattering—cannot be neglected in a physically realistic calculation. Although the unitarity bounds give an explicit indication of the importance of these rescattering terms in the region  $t \geq 4m_N^2$ , one has no reason to assume they are any less important in the region  $4m_K^2 \leq t \leq 4m_N^2$ . Whether rescattering effects increase or decrease the contribution from this region is not known at present, and one may only speculate. For example, the presence of a  $\phi(1020)$  resonance in the  $K\bar{K} \rightarrow N\bar{N}$  partial waves could, in principle, enhance the  $b_1^{\lambda_1, \lambda_2}$  from their BA values in some region of  $t$ . In fact, previous experience with  $\pi\pi$  contributions to nucleon isovector form factors suggests that rescattering may lead to enhanced low- $t$  contributions. In the work of Ref. [27], it was found that, in comparison to the BA contribution, rescattering contributions enhanced the  $t \leq 4m_N^2$  contribution to the isovector magnetic moment by roughly the same magnitude as the unitarity bounds reduced the  $t \geq 4m_N^2$  contribution.

Given the equivalence between the BA/PFF treatment of the dispersion relation and the one-loop contribution of Fig. 2(a), the results of the foregoing analysis should lead one to question the credibility of any one-loop prediction for the strangeness moments. Even model calculations which employ form factors to regulate the integrals do not include all of the rescattering corrections required by unitarity. Indeed, such form factors apply only to the meson-nucleon vertices, and not to the full  $K\bar{K} \rightarrow N\bar{N}$  (or  $KN \rightarrow KN$ ) scattering amplitude. Moreover, meson-nucleon form factors are often taken to be functions of  $k^2$ , where  $k_\mu$  is the four-momentum of the kaon, and are normalized to reproduce the SU(3) values for the meson-nucleon coupling when  $k^2 = m_K^2$ . Thus hadronic form factors have no impact on the BA violation of unitarity for scattering amplitudes in the physical region.

In a similar vein, we note that the use of a pointlike kaon strangeness form factor, as is used in most loop calculations reported to date, could represent as serious an error as the

violation of unitarity in the BA  $b_1^{\lambda_1, \lambda_2}$ . A comparison of the BA/U/PFF and BA/U/GS results in Table I shows that the inclusion of a reasonable parametrization of  $F_K^{(s)}(t)$ , displaying an enhancement in the vicinity of the  $\phi(1020)$ , can change magnitudes of  $\rho_D^s$  and  $\mu^s$  by as much as 30%. While our rationale for choosing such a parametrization is not based on any rigorous argument, we nevertheless believe that it constitutes a more realistic input than does the use of a pointlike form factor. We correspondingly expect most one-loop calculations employing the pointlike approximation to be physically unrealistic.

As a final observation, we make a comparison between the DR calculation and the one-kaon loop calculation of CHPT. To be concrete, we focus on the strangeness radius. Within the framework of CHPT, the only well-defined piece of a one-kaon loop contribution to  $\rho_D^s$  is that which is nonanalytic in the strange quark mass. The remaining piece is indistinguishable from tree-level contributions arising from the chiral Lagrangian, at a given order in the chiral scale,  $\Lambda_\chi \approx 4\pi f$ . Consequently, one subsumes all analytic contributions into the counterterms. In the case of  $\rho_D^s$ , only the amplitudes of Fig. 2(a) contribute a term nonanalytic in  $m_s$  at  $O(1/\Lambda_\chi^2)$ . Specifically, one finds [15]

$$\rho_D^s = \rho_{\text{loop}}^s - \left( \frac{2m_N}{\Lambda_\chi} \right)^2 c^s, \quad (51)$$

where

$$\rho_{\text{loop}}^s = \left( \frac{m_N}{\Lambda_\chi} \right)^2 \left\{ 1 + \frac{5}{3} \left[ \left( \frac{3F+D}{\sqrt{6}} \right)^2 + \frac{3}{2} (D-F)^2 \right] \right\} \times \left[ C_\infty - \ln \frac{m_K^2}{\mu^2} \right], \quad (52)$$

where  $C_\infty$  contains the UV regulator and  $\mu$  is the renormalization scale.<sup>2</sup> The counterterm  $c^s$  contains a piece canceling the UV divergence appearing in  $\rho_{\text{loop}}^s$  plus a finite remainder, containing all the analytic contributions at order  $1/\Lambda_\chi^2$ . The finite part of  $c^s$  can be further decomposed as

$$c^s = c_0 - 2[c_- - (c_+/3)], \quad (53)$$

where the  $c_\pm$  can be determined from the neutron and proton EM charge radii and where the constant  $c_0$  is associated with the SU(3) singlet current. It is the latter constant which cannot be determined from any existing data, since measurements have only been made of SU(3) octet vector current matrix elements. Consequently, CHPT cannot be used to make a model-independent prediction for  $\rho_D^s$ .

The correspondence between the results in Eqs. (51) and (52) and those obtained using the dispersion relation can be understood as follows. In the BA with a pointlike kaon form factor, one finds an identical  $\ln m_K^2$  IR singularity as that appearing in  $\rho_{\text{loop}}^s$ . The origin of this  $\ln m_K^2$  is a branch cut singularity in the BA partial waves for  $t \leq 4m_K^2(1 - m_K^2/4m_N^2)$  [31,32]. The dispersion relation result contains no renormalization scale dependence since the uni-

<sup>2</sup>In Ref. [15] contributions from  $\Sigma K$  intermediate states were also included, yielding the term proportional to  $(D-F)^2$  in Eq. (52). This contribution has been omitted in the present analysis.

tarity bound removes the UV divergence. As the nucleon mass is the only other scale which enters the calculation, one finds  $\mu \rightarrow m_N$  in the leading logarithmic contribution. Presumably, the remaining contributions in the BA, as well as those generated by resonant and nonresonant rescattering terms in the  $b_1^{\lambda_1, \lambda_2}$  (as necessitated by unitarity) and the effects of the physical  $F_K^{(s)}(t)$ , should be accounted for in CHPT by the counterterm  $c^s$ . Unfortunately, since  $c^s$  cannot be determined from existing data using symmetry, one must resort to other strategies for including the rescattering and  $F_K^{(s)}(t)$  effects.

## V. SUMMARY

In the present paper, we have made an initial study of the continuum contribution to the nucleon strangeness vector current form factors using the framework of dispersion relations. In focusing on the  $K\bar{K}$  contribution, we have illustrated how a leading order loop prediction for the strangeness radius and magnetic moment entails a substantial violation of unitarity. At the same time, we have derived a unitarity bound on this continuum contribution from the region in the dispersion integral above the  $N\bar{N}$  production threshold. Although we have specified our analysis to the case of the nonlinear SU(3)  $\sigma$  model, our conclusions regarding unitarity violation should hold for any chiral model which yields a similar structure for the  $K\bar{K} \rightarrow N\bar{N}$  scattering amplitude in the Born approximation. Our statement of the unitarity bound is general. We have also illustrated how the use of a reasonable, realistic kaon strangeness form factor can significantly affect one's predictions for  $\rho^s$  and  $\mu^s$ . We conclude that most model predictions for the two-kaon continuum contributions are physically unrealistic. We further suspect that our conclusions regarding the  $K\bar{K}$  intermediate state ought to apply as well to other leading order loop calculations, whether they involve higher-mass strange mesons and baryons, as in the quark model calculation of Ref. [26], or states containing three or more pseudoscalar mesons.

We emphasize that the contribution about which we have yet to make a definitive statement is the  $K\bar{K}$  contribution from the region below the  $N\bar{N}$  threshold. At present, the best we can do is make an estimate based on the BA for the  $b_1^{\lambda_1, \lambda_2}$  and a nonpointlike kaon strangeness form factor. The feasibility of making a refined analysis of this contribution by continuing fits to physical  $KN \rightarrow KN$  or  $K\bar{K} \rightarrow N\bar{N}$  scattering data will be discussed in a forthcoming study. Nevertheless, we are able to show how the contribution from this region to  $\rho_D^s$  can be significantly enhanced if the kaon strangeness form factor is strongly peaked in the vicinity of the  $\phi(1020)$ , as one would reasonably expect based on analogy with  $e^+e^- \rightarrow K\bar{K}$  data and on the flavor content of the lowest-lying  $0^-(1^{--})$  mesons. What remains to be resolved is the discrepancy between predictions for  $\rho_D^s$  using a VDM approach and those obtained using models for the continuum. The key may lie in a better understanding of the subthreshold behavior of the  $b_1^{\lambda_1, \lambda_2}$  as well as of the contribution from the three-pion continuum. Although it contains no valence strange quarks, the latter is the lightest state which may contribute to the DR's for  $F_1^{(s)}$  and  $F_2^{(s)}$ . The

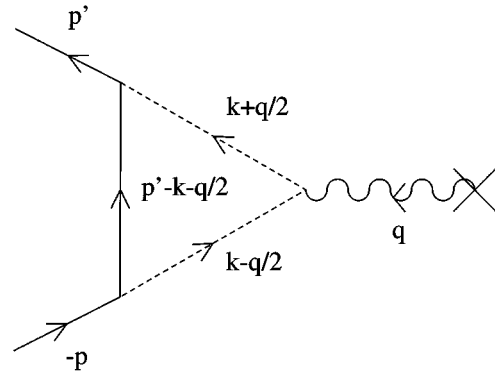


FIG. 9. Our choice of the internal and external momenta for the calculation of the imaginary parts arising from the  $t$ -channel discontinuity of the diagrams from Fig. 2(a).

scale of this contribution, along with those of  $N\bar{N}$  and  $B\bar{B}$  intermediate states, awaits the result of future work.

## ACKNOWLEDGMENTS

We wish to thank R.L. Jaffe, N. Isgur, and U.-G. Meissner for useful discussions. H.W.H. has been supported by the Deutsche Forschungsgemeinschaft (SFB 201) and the German Academic Exchange Service (Doktorandenstipendium HSP II/ AUFE). M.J.M. has been supported in part under U.S. Department of Energy Contracts Nos. DE-FG06-90ER40561 and DE-AC05-84ER40150 and through the National Science Foundation Young Investigator program.

## APPENDIX: IMAGINARY PARTS TO ONE LOOP

We show here the equivalence between the one-loop diagrams of Fig. 2(a) and the Born approximation for the  $KN$  scattering amplitudes in conjunction with the dispersion relation approach [see Fig. 3(a)]. To that end, we calculate the imaginary part of the one-loop diagrams from Fig. 2(a) which arises from the  $t$ -channel discontinuity. The equality is then easily checked by comparing our results with Eqs. (41) and (42). It does not depend on one's choice for the kaon strangeness form factor. For simplicity, we therefore assume pointlike kaons. Any nonpointlike kaon strangeness form factor would simply multiply the resulting spectral functions.

In the following, we refer to the diagram with the propagating  $\Lambda$  (the triangle diagram) as diagram (1). We assign the momenta to the particle lines as shown in Fig. 9. For the other diagram with the kaon loop [referred as diagram (2)], we assign the momenta in the same way and leave out the  $\Lambda$  momentum. Since we produce a nucleon-antinucleon pair,  $q$  has to be timelike, i.e.,  $q^2 = t \geq 0$ . We work in the center-of-momentum frame of the nucleon-antinucleon pair, where  $q = (\omega, \vec{0})$ . Using momentum conservation, we have  $p' = (\omega/2, \vec{p}')$  and  $p = (\omega/2, -\vec{p}')$  with  $|\vec{p}'| = P = \sqrt{t/4 - m_N^2}$ . We define the contribution of a particular Feynman diagram to the vertex function  $\Gamma_\mu$  by

$$\mathcal{M}_\mu^{(i)} = -i\bar{U}(p')\Gamma_\mu^{(i)}V(p), \quad (\text{A1})$$

where the strangeness charge of the kaons  $Q_s \equiv -1$  has been absorbed in  $\Gamma_\mu^{(i)}$ . Using the nonlinear SU(3)  $\sigma$  model and calculating the isoscalar contribution, we obtain the following contributions to the vertex functions:

$$\Gamma_{\mu}^{(1)} = iQ_s \frac{(3F+D)^2}{6f^2} \int \frac{d^4k}{(2\pi)^4} \frac{k_{\mu}(k+q/2)(p'-k-q/2-m_{\Lambda})(k-q/2)}{[(k-q/2)^2-m_K^2+i\epsilon][(k+q/2)^2-m_K^2+i\epsilon][(p'-k-q/2)^2-m_{\Lambda}^2]}, \quad (\text{A2})$$

$$\Gamma_{\mu}^{(2)} = iQ_s \frac{3}{f^2} \int \frac{d^4k}{(2\pi)^4} \frac{k_{\mu}k}{[(k-q/2)^2-m_K^2+i\epsilon][(k+q/2)^2-m_K^2+i\epsilon]}. \quad (\text{A3})$$

Since the denominator of the  $\Lambda$  propagator does not vanish in the  $t$ -channel physical region, the  $i\epsilon$  can be dropped. The  $\Gamma_{\mu}^{(i)}$  have branch cuts on the real axis for  $t \geq 4m_K^2$ . We calculate now the imaginary parts stemming from the discontinuity associated with these cuts:

$$\text{Im}\Gamma^{\mu} = \frac{1}{2i} \Delta\Gamma^{\mu} = \frac{1}{2i} \lim_{\delta \rightarrow 0} [\Gamma^{\mu}(\omega+i\delta) - \Gamma^{\mu}(\omega-i\delta)]. \quad (\text{A4})$$

It is convenient to use the so-called Cutkosky rules [50,51], which give a compact expression for the discontinuities associated with physical region singularities of Feynman amplitudes. In particular, we obtain the discontinuities  $\Delta\Gamma_{\mu}^{(i)}$  by cutting the kaon lines in diagrams (1) and (2) and replacing their propagators by  $\delta$  functions (A5),

$$\frac{1}{p^2-m^2+i\epsilon} \rightarrow -2\pi i \theta(p_0) \delta(p^2-m^2). \quad (\text{A5})$$

As a consequence, the discontinuity arises for the intermediate particles on the mass shell. Note the equivalence to the dispersion relation approach, in which the intermediate states are also on shell. Because of the  $\delta$  functions, the  $d^4k$  integration now covers only a finite part of the  $k$  space, leading to a finite value of the integral. Consequently, the divergences of the integrals, Eqs. (A2) and (A3), do not contribute to the discontinuity across the cut. The imaginary part is finite, and only the real part has to be regulated. Next we write  $d^4k$  as  $dk_0 k^2 dk d\Omega_k$  and use the  $\delta$  functions to carry out the  $dk_0$  and  $dk$  integrations. As a consequence, we obtain  $k=(0, \vec{k})$  with  $|\vec{k}|=Q=\sqrt{t/4-m_K^2}$ . Moreover, the  $d\Omega_k$  integration involves only the cosine  $x$  of the angle between  $\vec{k}$  and  $\vec{p}'$ . We obtain

$$\text{Im}\Gamma_{\mu}^{(1)} = Q_s \frac{(3F+D)^2}{48\pi f^2} \frac{Q}{\sqrt{t}} \frac{1}{2} \int_{-1}^1 dx \left( k_{\mu}(k+2\vec{M}) - \frac{2\vec{M}^2}{PQ} \frac{k_{\mu}(k+m_N\vec{M}\vec{\Delta}\vec{M})}{x_B-x} \right), \quad (\text{A6})$$

$$\text{Im}\Gamma_{\mu}^{(2)} = -Q_s \frac{3}{8\pi f^2} \frac{Q}{\sqrt{t}} \frac{1}{2} \int_{-1}^1 dx k_{\mu}k, \quad (\text{A7})$$

where

$$x_B = \frac{t-2m_K^2+4m_N\vec{M}\vec{\Delta}\vec{M}}{4PQ} > 1. \quad (\text{A8})$$

Finally,  $\text{Im}\Gamma_{\mu}^{(i)}$  can be expressed in terms of the integrals

$$L_{\mu} = \frac{1}{2} \int_{-1}^1 dx k_{\mu}, \quad (\text{A9})$$

$$L_{\mu\nu} = \frac{1}{2} \int_{-1}^1 dx k_{\mu}k_{\nu}, \quad (\text{A10})$$

$$I_{\mu} = \frac{1}{2} \int_{-1}^1 dx \frac{k_{\mu}}{x_B-x}, \quad (\text{A11})$$

$$I_{\mu\nu} = \frac{1}{2} \int_{-1}^1 dx \frac{k_{\mu}k_{\nu}}{x_B-x}, \quad (\text{A12})$$

and these integrals can be decomposed into  $g_{\mu\nu}$  and symmetrical combinations of the independent four-vectors  $\Delta=(p'-p)/2$  and  $q=p+p'$ . Their coefficients can be obtained in a standard manner by evaluating the integrals  $q_{\mu}I^{\mu}$ ,  $\Delta_{\mu}I^{\mu}$ , and so on. Furthermore, the  $I$  integrals can be expressed through Legendre functions of the second kind. For example, we find

$$I_{\mu\nu} = \frac{1}{3} Q^2 [Q_2(x_B) - Q_0(x_B)] g_{\mu\nu} - \frac{1}{3} \frac{Q^2}{t} \times [Q_2(x_B) - Q_0(x_B)] q_{\mu}q_{\nu} + \frac{Q^2}{P^2} Q_2(x_B) \Delta_{\mu}\Delta_{\nu}. \quad (\text{A13})$$

Using the relation

$$\text{Im}\Gamma_{\mu}^{(i)} = \gamma_{\mu} \text{Im}F_1^{(i)} + i \frac{\sigma_{\mu\nu}}{2m} q^{\nu} \text{Im}F_2^{(i)}, \quad (\text{A14})$$

we can identify the contributions to the imaginary parts of the Dirac and Pauli form factors for  $t \geq 4m_N^2$ , respectively. We add now the contributions of the two diagrams and the spectral functions emerge as

$$\text{Im}F_1^{(s)}(t) = \frac{Q_s}{24\pi f^2} \frac{Q^3}{\sqrt{t}} \left\{ \frac{3}{2} - \frac{1}{6} (3F+D)^2 + \frac{1}{3} (3F+D)^2 \left( \frac{\vec{M}^2}{PQ} \right) [Q_0(x_B) - Q_2(x_B)] - (3F+D)^2 \frac{m_N^2}{P^2} \left[ \left( \frac{\vec{M}^2}{PQ} \right) Q_2(x_B) + \left( \frac{\vec{M}^2 \Delta \vec{M}}{Q^2} \right) Q_1(x_B) \right] \right\}, \quad (\text{A15})$$

$$\text{Im}F_2^{(s)}(t) = \frac{Q_s}{24\pi f^2} \frac{Q^3}{\sqrt{t}} (3F+D)^2 \frac{m_N^2}{P^2} \left\{ \left( \frac{\bar{M}^2}{PQ} \right) Q_2(x_B) + \left( \frac{\bar{M}^2 \Delta \bar{M}}{Q^2} \right) Q_1(x_B) \right\}. \quad (\text{A16})$$

Up to the kaon strangeness form factor, these expressions are exactly the same as obtained by the Born approximation for

the  $b_1^{\lambda_1, \lambda_2}$  and the dispersion relation approach [compare with Eqs. (41) and (42)]. The imaginary parts, Eqs. (A15) and (A16), are defined for  $t \geq 4m_N^2$ . Since the discontinuity starts at  $4m_K^2$ , they have to be analytically continued into the unphysical region  $4m_K^2 \leq t < 4m_N^2$ . This is easily done by replacing the momentum  $P = \sqrt{t/4 - m_N^2}$  by  $ip_- = i\sqrt{m_N^2 - t/4}$ . Consequently, the variable  $x_B$  becomes complex ( $x_B \rightarrow -i\xi_B$ ), and the Legendre functions of the second kind have to be analytically continued, too.

- 
- [1] M. J. Musolf *et al.*, Phys. Rep. **239**, 1 (1994).  
[2] CCFR, A. O. Bazarko *et al.*, Z. Phys. C **65**, 189 (1995); CCFR, S. A. Rabinowitz *et al.*, Phys. Rev. Lett. **70**, 134 (1993).  
[3] MIT-Bates proposal No. 89-06, 1989, R. D. McKeown and D.H. Beck, spokespersons.  
[4] MIT-Bates proposal No. 94-11, 1994, M. Pitt and E. J. Beise, spokespersons.  
[5] CEBAF proposal No. PR-91-017, 1991, D. H. Beck, spokesperson.  
[6] CEBAF proposal No. PR-91-004, 1991, E. J. Beise, spokesperson.  
[7] CEBAF proposal No. PR-91-010, 1991, M. Finn and P. A. Souder, spokespersons.  
[8] Mainz proposal No. A4/1-93, 1993, D. von Harrach, spokesperson.  
[9] Los Alamos proposal No. 1173, W.C. Louis, spokesperson.  
[10] K.-F. Liu, University of Kentucky Report No. UK/95-11, 1995 (unpublished) and references therein.  
[11] D. B. Leinweber, Phys. Rev. D **53**, 5115 (1996).  
[12] EMC, J. Ashman *et al.*, Nucl. Phys. **B328**, 1 (1989); E142 Collaboration, P. L. Anthony *et al.*, Phys. Rev. Lett. **71**, 959 (1993); SMC, B. Adeva *et al.*, Phys. Lett. B **302**, 533 (1993); SMC, D. Adams *et al.*, Phys. Lett. B **329**, 399 (1994); E143 Collaboration, K. Abe *et al.*, Phys. Rev. Lett. **74**, 346 (1995).  
[13] E. J. Beise (private communication).  
[14] J. Donoghue, E. Golowich, and B. Holstein, *Dynamics of the Standard Model* (Cambridge University Press, Cambridge, England, 1992); in *Proceedings of the Workshop on Effective Theories of the Standard Model*, edited by U.-G. Meissner (World Scientific, Singapore, 1992).  
[15] M. J. Musolf and H. Ito, INT Report Nos. DOE/ER/40561-245-INT96-00-114, nucl-th/9607021 (unpublished).  
[16] R. L. Jaffe, Phys. Lett. B **229**, 275 (1989).  
[17] H.-W. Hammer, U.-G. Meissner, and D. Drechsel, Phys. Lett. B **367**, 323 (1996).  
[18] M. J. Musolf and M. Burkardt, Z. Phys. C **61**, 433 (1994).  
[19] W. Koepf, S. J. Pollock, and E. M. Henley, Phys. Lett. B **288**, 11 (1992); W. Koepf and E. M. Henley, Phys. Rev. C **49**, 2219 (1994).  
[20] H. Forkel *et al.*, Phys. Rev. C **50**, 3108 (1994).  
[21] T. Cohen, H. Forkel, and M. Nielsen, Phys. Lett. B **316**, 1 (1993).  
[22] N. W. Park, J. Schechter, and H. Weigel, Phys. Rev. D **43**, 869 (1991).  
[23] S.-T. Hong and B.-Y. Park, Nucl. Phys. **A561**, 525 (1993).  
[24] S. C. Phatak and S. Sahu, Phys. Lett. B **321**, 11 (1994).  
[25] H. Ito, Phys. Rev. C **52**, R1750 (1995).  
[26] P. Geiger and N. Isgur, Phys. Rev. D **55**, 299 (1997).  
[27] P. Federbush, M. L. Goldberger, and S. B. Treiman, Phys. Rev. **112**, 642 (1958).  
[28] G. F. Chew *et al.*, Phys. Rev. **110**, 265 (1958).  
[29] W. R. Frazer and J. R. Fulco, Phys. Rev. **117**, 1603 (1960); **117**, 1609 (1960).  
[30] G. Höhler *et al.*, Nucl. Phys. **B114**, 505 (1976).  
[31] P. Mergell, U.-G. Meissner, and D. Drechsel, Nucl. Phys. **A596**, 367 (1996); H.-W. Hammer, U.-G. Meissner, and D. Drechsel, Phys. Lett. B **385**, 343 (1996).  
[32] S.D. Drell and F. Zachariasen, *Electromagnetic Structure of Nucleons* (Oxford University Press, New York, 1960).  
[33] R. G. Sachs, Phys. Rev. **126**, 2256 (1962).  
[34] We are indebted to R.L. Jaffe for emphasizing this point.  
[35] M. Jacob and G. C. Wick, Ann. Phys. (N.Y.) **7**, 404 (1959).  
[36] Since the reaction  $K\bar{K} \rightarrow N\bar{N}$  is an inelastic one, a partial wave expansion of the  $S$ -matrix element is equivalent to a partial wave expansion of the corresponding  $T$ -matrix element, up to constant factors.  
[37] S. Fubini, Y. Nambu, and V. Wataghin, Phys. Rev. **111**, 329 (1958), Appendix II.  
[38] See, e.g., J. L. Basdevant, C. D. Froggatt, and J. C. Petersen, Nucl. Phys. **B72**, 413 (1974); W. Männer, presented at the 17th Conference on high-energy physics, London, 1974 (unpublished).  
[39] W. R. Frazer and J. R. Fulco, Phys. Rev. Lett. **2**, 365 (1959).  
[40] G. Höhler and E. Pietarinen, Nucl. Phys. **B95**, 210 (1975).  
[41] See, e.g., M. F. Heyn and C. B. Lang, Z. Phys. C **7**, 169 (1981).  
[42] G. Ecker *et al.*, Phys. Lett. B **223**, 425 (1989); G. Ecker *et al.*, Nucl. Phys. **B321**, 311 (1989).  
[43] Particle Data Group, R. M. Barnett *et al.*, Phys. Rev. D **54**, 1 (1996).  
[44] B. Delcourt *et al.*, Phys. Lett. **99B**, 257 (1981); F. Mané *et al.*, *ibid.* **99B**, 261 (1981); J. Buon *et al.*, **118B**, 221 (1982).  
[45] F. Felicetti and Y. Srivastava, Phys. Lett. **107B**, 227 (1981).  
[46] G. J. Gounaris and J. J. Sakurai, Phys. Rev. Lett. **21**, 244 (1968).  
[47] H. Georgi, *Weak Interactions and Modern Particle Theory* (Benjamin/Cummings, Menlo Park, CA, 1984), Chaps. 5 and 6.  
[48] In the present context, we avoid making the heavy baryon expansion of the nonlinear chiral Lagrangian, even though such an expansion provides a well-defined truncation scheme for baryon CHPT with loops. For  $KN$  scattering in the BA,

however, the heavy baryon Lagrangian does not yield the correct pole structure.

- [49] Such suppression may not hold in the real world. See, e.g., E. Hirsch *et al.*, Phys. Lett. **36B**, 139 (1971); E. Hirsch, U. Karshon, and H. J. Lipkin, *ibid.* **36B**, 385 (1971).
- [50] R. E. Cutkosky, J. Math. Phys. (N.Y.) **1**, 429 (1960).
- [51] See, e.g., C. Itzykson and J.-B. Zuber, *Quantum Field Theory* (McGraw-Hill, New York, 1980).